CDDpress

www.nature.com/cdd

ARTICLE

Check for updates

iASPP suppression mediates terminal UPR and improves BRAF-inhibitor sensitivity of colon cancers

Shanliang Zheng[1,3], Xingwen Wang[1,3], Hao Liu[1], Dong Zhao[1], Qingyu Lin[1], Qinghua Jiang[1], Li Li[2]✉ and Ying Hu[1]✉

Unfolded protein response (UPR) signaling is activated under endoplasmic reticulum (ER) stress, an emerging cancer hallmark, leading to either adaptive survival or cell death, while the mechanisms underlying adaptation-death switch remain poorly understood. Here, we examined whether oncogene iASPP regulates the switch and how the mechanisms can be used in colon cancer treatment. iASPP is downregulated when cells undergo transition from adaptation to death during therapy-induced ER stress. Blocking iASPP's downregulation attenuates stress-induced cell death. Mechanistically, Hu-antigen R (HuR)-mediated stabilization of iASPP mRNA and subsequent iASPP protein production is significantly impaired with prolonged ER stress, which facilitates the degradation of GRP78, a key regulator of the UPR, in the cytosol. Because iASPP competes with GRP78 in binding the ER-resident E3 ligase RNF185, and tips the balance in favor of cell death. Positive correlation between the levels of HuR, iASPP, and GRP78 are detectable in colon cancer tissues in vivo. Genetic inhibition of iASPP/GRP78 or chemical inhibition of HuR not only inhibits tumor growth, but also sensitizes colon cancer cells' responses to BRAF inhibitor-induced ER stress and cell death. This study provides mechanistic insights into the switch between adaptation and death during ER stress, and also identifies a potential strategy to improve BRAF-inhibitor efficiency in colon cancers.

Cell Death & Differentiation (2023) 30:327–340; https://doi.org/10.1038/s41418-022-01086-w

INTRODUCTION

Cancer cells are constantly subjected to intrinsic and extrinsic stresses, many of which can disrupt endoplasmic reticulum (ER) homeostasis by inducing the accumulation of misfolded proteins inside the ER [1, 2]. To cope with ER stress, cells have evolved elegant mechanisms to sense the intensity and duration of a stress, with the intention of mitigating it via an integrated signal transduction pathway termed the unfolded protein response (UPR) [3]. However, if ER stress cannot be resolved, the UPR leads to cell death (terminal UPR) [4]. Although increased ER stress normally facilitates adaptive survival in cancer cells, it can be exploited for cancer treatment [5]. As such, increased knowledge about how cells switch between the two divergent UPR signaling outputs, adaptation or cell death, is urgently needed because it may offer new opportunities to tip the balance toward cell death, inhibiting tumor growth and improving treatment efficiency. In mammalian cells, the UPR is initiated by three sensors embedded in the ER membrane: activating transcription factor 6 [6], inositol-requiring enzyme 1α (IRE1α) [7], and PRKR-like ER kinase [8]. Under non-stressed conditions, GRP78 is constitutively bound to the three sensors, preventing their activation [4]. Upon ER stress, GRP78 preferentially binds to unfolded proteins, so that the three sensors are rapidly activated and transduce stress signals to the cytosol and nucleus [3]. Paradoxically, the UPR signals simultaneously activate both survival and cell-death effectors [9]. It is known that the activation of ER chaperones, such as GRP78, or transient attenuation of protein translation can facilitate stress adaptation during the UPR, while the activation of CCAAT-enhancer-binding protein homologous protein (CHOP) and c-Jun N-terminal kinase (JNK), and the modulation of Bcl-2-family components facilitate the induction of apoptosis [10–13]. Efforts have been made to understand the binary switch process between life and death. For example, DNA damage-responsive pro-apoptotic factor E2F1 has been shown to regulate the cell survival/death decision under ER stress [14]. However, the underlying mechanisms that turn off adaptation and engage proapoptosis are still unclear and the potential applications of such mechanisms in the context of cancer treatment are underexplored.

Inhibitor of Apoptosis Stimulating Protein of P53 (iASPP) is an oncogene. Increased iASPP expression is associated with drug resistance and predicts poor prognosis in patients with colon, liver and breast cancer, renal cell carcinoma, and leukemia [15–18]. Previous studies revealed that iASPP, despite known as a p53 inhibitor [19], has been shown to inhibit apoptosis by promoting the activity of the antioxidative transcription factor Nrf2 in a p53-indepedent manner [15]. It can also coordinate with a newly reported calcium channel protein, TMCO1 (Transmembrane and Coiled-Coil Domains 1), to maintain low basal ER calcium levels in cancer cells [20]. Of note, both oxidative stress and changes in calcium homeostasis can trigger ER stress leading to the UPR [21, 22]. The connections between these processes and iASPP

[1]School of Life Science and Technology, Harbin Institute of Technology, Harbin, Heilongjiang Province 150001, China. [2]The third affiliated hospital of Harbin Medical University, Harbin, Heilongjiang Province 150040, China. [3]These authors contributed equally: Shanliang Zheng, Xingwen Wang. ✉email: 920221984@qq.com; huying@hit.edu.cn

Edited by M. Bianchi

Received: 30 June 2022 Revised: 23 October 2022 Accepted: 1 November 2022
Published online: 15 November 2022

have motivated us to further investigate iASPP's ability to influence UPR signaling outputs.

Our data revealed a HuR-iASPP-RNF185/GRP78 axis, which is increased in colon cancers. Chemical inhibition of HuR or genetic inhibition of iASPP-GRP78 not only inhibited tumor growth, but also sensitized colon cancers to BRAF inhibitor-induced ER stress and cell death both in vitro and in vivo. Thus, we present a mechanistic explanation for the switch from adaptation to cell death under prolonged ER stress, and also demonstrate its potential significance in improving the responses of colon cancers to BRAF inhibitors.

RESULTS

Dynamic changes in iASPP expression define the switch from initial adaptation to terminal UPR in response to ER stress

To understand whether iASPP regulates the UPR, we treated two colon cancer cell lines, HT-29 and HCT-116, for the indicated durations with two well-established ER-stress inducers: thapsigargin (TG), an inhibitor of SERCAs, and tunicamycin (TN), an *N*-linked protein glycosylation inhibitor. Cell viability assays revealed that shorter-term (0–12 h) exposure to TG or TN elicited no obvious toxic effects. Significant reductions in cell viability were detected 18 and 24 h after TG or TN exposure in a time-dependent manner, as revealed by both crystal violet staining and MTT (3-[4,5-dimethylthiazol-2-yl]-2,5 diphenyl tetrazolium bromide) assays (Figs. 1A and S1A). We defined short-term treatment (0–12 h) as the adaptive phase and 18–24 h as the terminal phase. Activation of the UPR was confirmed by increase in GRP78 and ATF6 proteins, and phosphorylation of PERK and IRE1, and their downstream factors, ATF4 and XBP1s (Figs. 1B and S1B, C). Only with longer treatment times, iASPP levels started to decline, which was coincided with the switch from adaptation to the terminal UPR (Fig. 1B). In addition, KEGG pathway enrichment analysis of different expression genes after iASPP overexpression identified protein processing in endoplasmic reticulum as one of top pathways (Fig. 1C). The following Gene set enrichment analysis (GSEA) was performed with the gene set of protein processing in ER in the control vs. iASPP overexpression and revealed a significant correlation between iASPP expression and protein processing in ER (Fig. 1D). Similar results were obtained when we divided the samples of colon cancer TCGA dataset into iASPP high and low groups using the medium level of iASPP as a threshold (Fig. S1D). These results inspired us to investigate whether iASPP regulates ER stress and whether the dynamic changes of iASPP during ER stress is essential for the shift from adaptation to death during ER stress. To do this, we restored iASPP expression in ER-stressed colon cancer cells. Strikingly, restoration of iASPP expression similar to the basal level completely abolished ER stress-induced cell death (Figs. 1E, F, S1E). Similar kinetic changes of iASPP expression were observed in cell lines derived from other cancer types during ER stress, such as bladder (T24) and cervical (HeLa) cancers (Fig. S1F, G). In these cells, iASPP downregulation coincided with increased cell death (Fig. S1H), while restoration of iASPP expression abrogated ER-stress-induced cell death (Fig. S1I–K). Thus, iASPP downregulation controls cellular switching from initial adaptation to cell death under ER-stress conditions.

iASPP regulates the switch by stabilizing the central UPR regulator GRP78

We then sought to understand how iASPP controls the switch under ER stress. We noted that the downregulation of iASPP expression occurred at the same time as decreased expression of GRP78 protein, a key upstream regulator of UPR sensors, during the terminal phase (Fig. 1B). The coordinated changes of other UPR markers were not evident (Fig. S1B). In addition, GRP78 recovery suppressed switching from adaptation to death (Fig. S1L–N). By contrast, GRP78 knockdown (KD) promoted ER stress-induced cell death and completely abrogated the effect of iASPP overexpression (Figs. 2A and S2A).

We then explored whether iASPP directly regulates GRP78 expression. As shown, ectopic expression of iASPP increased GRP78 protein levels, while inhibition of endogenous iASPP decreased them (Fig. 2B). The impacts of iASPP on GRP78 are likely specific, because GRP94 or protein disulphide isomerase (PDI), which also play roles in proper protein folding in ER lumen, were not changed by iASPP expression (Fig. 2B). iASPP had no obvious effects on GRP78 mRNA levels (Fig. S2B). Instead, the proteasome inhibitor MG132 completely abolished the effect of iASPP on GRP78 expression (Fig. 2C), while the lysosome inhibitor CQ had no effect (Fig. S2C). In addition, the half-life of GRP78 was prolonged from about 2 to 8 h by iASPP expression in HT-29 cells (Fig. 2D).

To understand whether and how iASPP regulates GRP78, the kinetics of GRP78 mRNA and protein were first examined after triggering ER stress. As shown, GRP78 mRNA levels increased at 6 h and reached a plateau 12 h after TG treatment, a point at which both iASPP and GRP78 protein levels were visibly reduced and cell viability had declined significantly (Fig. 2E). Therefore, although likely to contribute, elevated GRP78 mRNA expression is unlikely to be the main reason for the dramatic decrease of GRP78 protein levels seen with prolonged TG treatment. Of note, MG132 (but not CQ) treatment rescued TG-induced GRP78 inhibition 24 h after TG exposure (Figs. 2F and S2D). In addition, GRP78 was also found to be polyubiquitinated, as indicated by higher molecular bands/smears in an immunoprecipitation (IP) assays of cultured colon cancer cells, and levels of polyubiquitinated GRP78 were increased by prolonged TG treatment (Fig. S2E). Recovery of iASPP expression reduced the levels of polyubiquitinated GRP78 and also restored GRP78 expression in the terminal phase (Fig. 2G). Thus, iASPP downregulation leads to increased GRP78 protein turnover, which facilitates the switch from adaptation to cell death during prolonged ER stress.

GRP78 is a novel substrate of RNF185

We went on to ask how GRP78 protein stability is regulated and found that genetic KD of RNF185, but not of the other ER-localized E3 ligases (Gp78, RNF5, HRD1, and TMEM129), increased GRP78 levels (Fig. S3A). This effect was validated using independent siRNA oligonucleotides that specifically target RNF185 (Fig. 3A). By contrast, overexpression of wild-type (WT) RNF185, but not an RNF185 E3 ligase activity-defective mutant (RNF185 C39A), reduced GRP78 levels (Fig. 3A). Consistently, WT RNF185 increased GRP78 polyubiquitination, while RNF185 C39A did not (Fig. S3B). In addition, RNF185 overexpression-mediated GRP78 polyubiquitination was detected in the presence of at cysteine (K)48, but not K33 or K63 (Fig. S3C). An ubiquitin mutant K48R prevented the formation of GRP78 ubiquitin chains (Fig. 3B). RNF185 KD almost completely abolished GRP78 polyubiquitination at K48 (Fig. 3B) and increased the protein half-life (Fig. 3C).

These data outlined above suggest that GRP78 may be a novel substrate of RNF185, in which case, GRP78, and RNF185 should bind with each other. Indeed, an IP assay revealed that GRP78 forms a complex with RNF185 in HT-29 cells (Fig. 3D). Their direct interaction was further validated in vitro using purified GRP78 and RNF185 (Fig. 3E, F). In addition, the N-terminus of GRP78 contains a GTPase domain that is required for its binding with RNF185 (Fig. 3E). A ring domain-containing RNF185 mutant bound to GRP78 as efficiently as full-length GRP78, while RNF185 mutant that did not have the ring domain failed to bind (Fig. 3F). In addition, the direct interaction between GRP78 and RNGF185 was further validated by Proximity Ligation Assay (PLA) (Fig. 3G). Their interaction was increased by TG. RING domain defective RNF185 mutant lost its binding ability with GRP78 (Fig. 3G).

In support of above idea that RNF185 is a key E3 ligase to induce GRP78 degradation, GRP78 was found to be localized

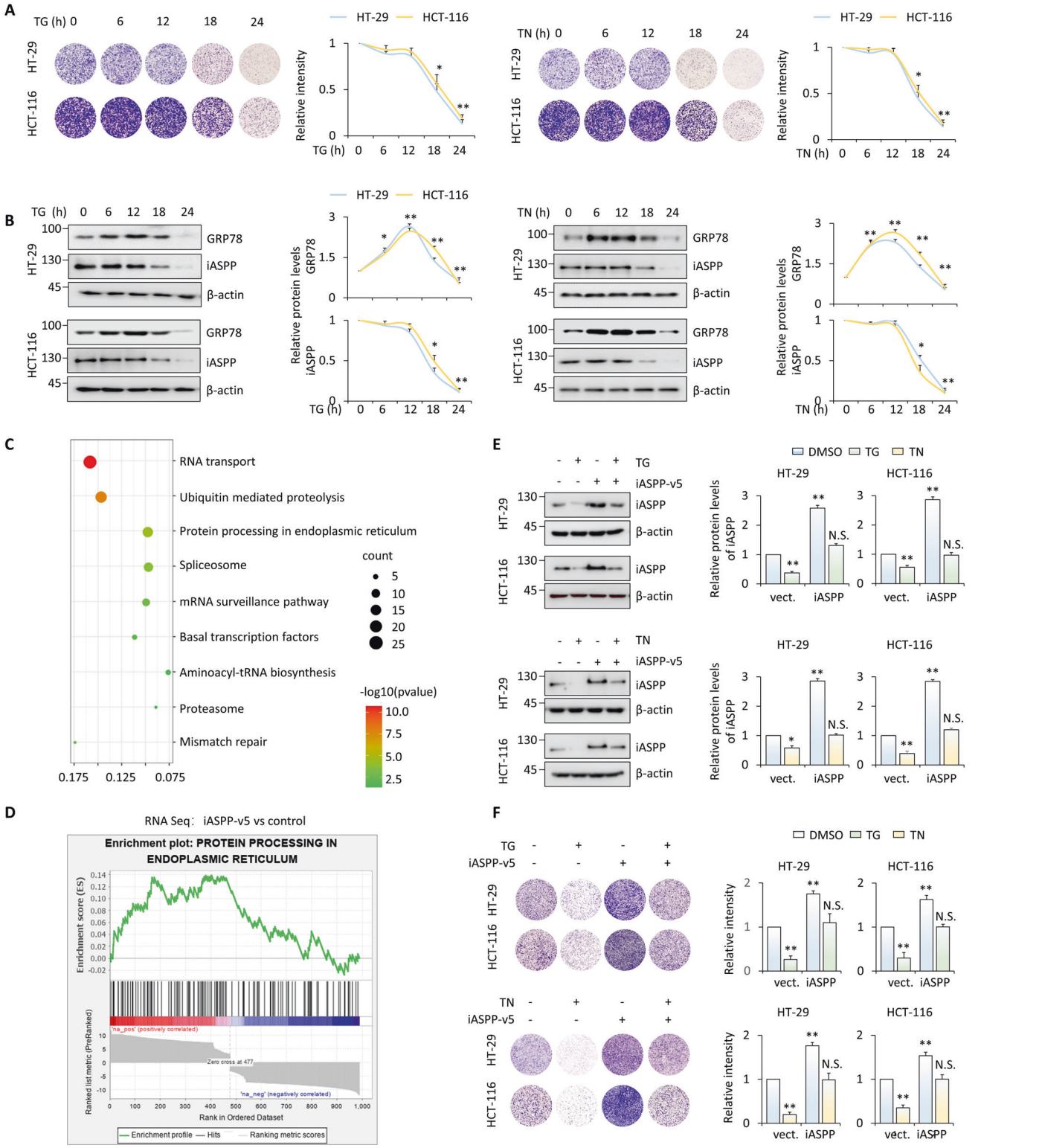

Fig. 1 Dynamic changes in iASPP expression define the switch. Representative crystal violet staining images of HT-29 and HCT-116 cells treated with Thapsigargin (TG, 2 μg/mL) or Tunicamycin (TN, 2 μM) in indicated time durations (**A**) or after transfected with iASPP-v5 followed by 24 h of TN or TG treatments (**F**). The images were quantified by image J and the data were plotted in the graphs (right). **B**, **E** Representative western blot images of GRP78 and iASPP protein in HT-29 and HCT-116 cells with the same treatments as described above. β-actin was used as a loading control. The bands were quantified by image J and the data were plotted in the graphs (right). KEGG pathway enrichment analysis (**C**) and Gene set enrichment analysis (**D**) were performed after iASPP overexpression in HCT-116 cells. Values in the control groups were normalized to 1. N.S. not significant $^{*}P < 0.05$; $^{**}P < 0.01$.

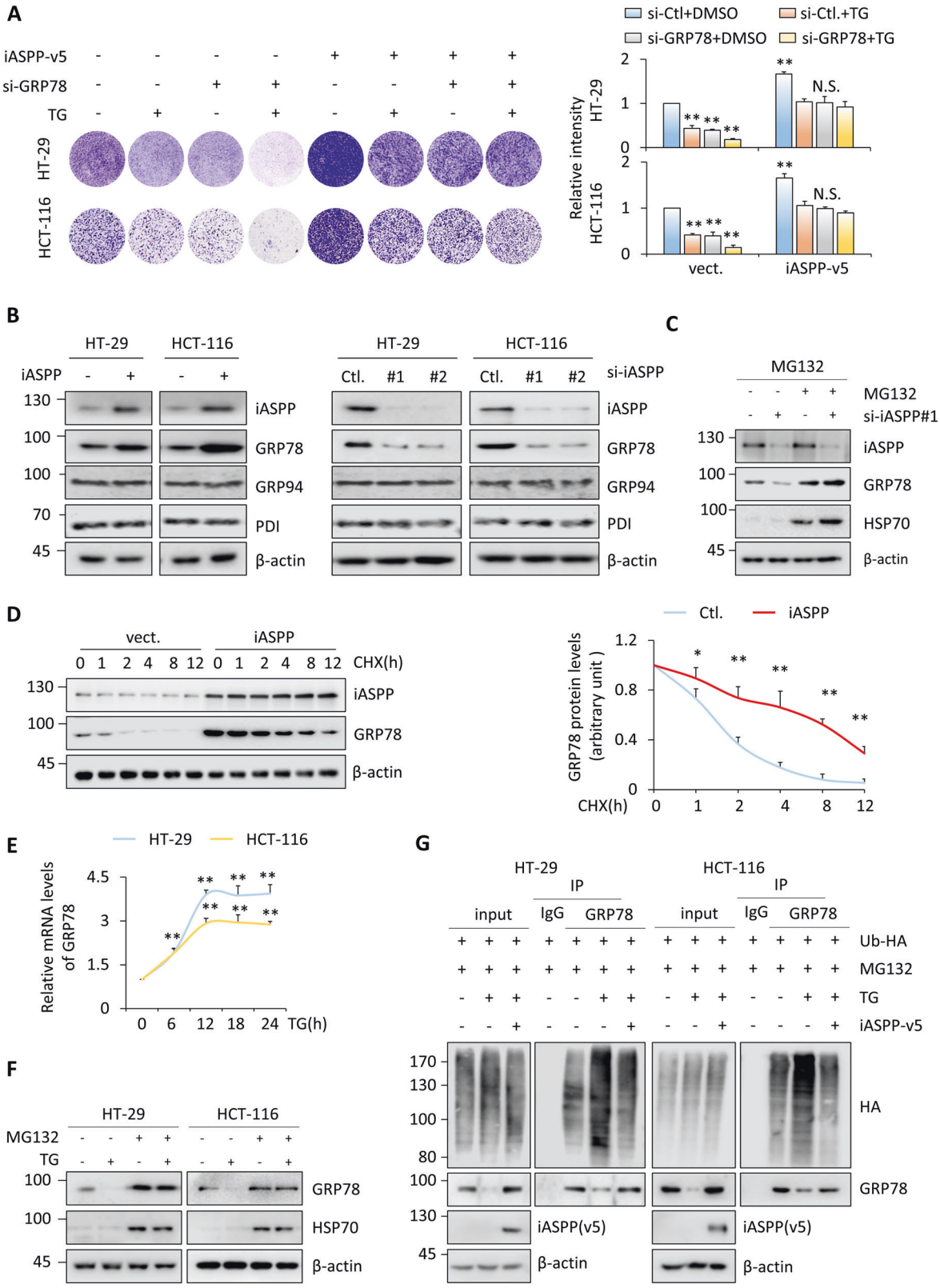

in both cytosol and the ER lumen, as revealed by cell permeabilization assay (Fig. 3H, I). Intriguingly, the cytosolic fraction was more sensitive to TG-induced GRP78 decrease (Fig. 3H, I). RNF185 KD or MG132 treatment prevented the effect of TG (Fig. 3H, I). ER fractionation assay also demonstrated that cytoplasmic localization of GRP78 can be restored by MG132 (Fig. S3D). Therefore, RNF185 promotes the degradation of GRP78 in the cytosol.

Furthermore, GRP78 ubiquitination at K447 was reported previously in a mass spectrometry screening study [23]. Our data

Fig. 2 iASPP regulates the switch by stabilizing GRP78. A Representative crystal violet staining images of HT-29 and HCT-116 cells with the indicated treatments. The images were quantified by image J and the data were plotted in the graphs (right). Representative western blot images of iASPP, GRP78, GRP94 and PDI protein in cells after iASPP knocking down (KD) or overexpression (OE) (**B**), iASPP KD combined with proteasome inhibitor MG132 (40 μM) (**C**), or iASPP OE combined with 100 μg/mL CHX treatment in indicated time durations (**D**) in HT-29 and/or HCT-116 cells. β-actin was used as a loading control. **E** The mRNA levels of GRP78 were measured by qRT-PCR assays after treated with 2 μg/mL TG in indicated time in HT-29 and HCT-116 cells. **F** Representative western blot images of GRP78 and iASPP protein in HT-29 and HCT-116 cells after treated with TG and/or MG132. β-actin was used as a loading control. **G** GRP78 ubiquitination (Ub-GRP78) was determined in HT-29 and HCT116 cells by immunoprecipitation (IP) of GRP78 followed by western blot of anti-HA after transfection of iASPP-v5 and Ubiquitin (Ub)-HA followed by TG treatment in the presence of MG132 (20 μM). β-actin was used as a loading control. The staining images (**A**) and western blots bands (**D**) were quantified by Image J and Values in the control groups were normalized to 1. N.S., not significant $^{*}P < 0.05$; $^{**}P < 0.01$ (**A**, **D**, **E**).

also show that the GRP78 K447A mutant completely lost its ability to be ubiquitinated (Fig. 3J). In addition, unlike WT GRP78, GRP78 K447A levels did not change with RNF185 overexpression or TG treatment (Fig. 3K, L). Therefore, RNF185 binds directly to GRP78 at its GTPase domain through its ring domain, and induces polyubiquitination of GRP78 at K447 in the cytosol under prolonged ER stress, leading to proteasome-mediated GRP78 protein degradation.

iASPP disrupts the binding between RNF185 and GRP78

iASPP-regulated stabilization of GRP78 was completely abolished by RNF185 KD (Fig. 4A). However, iASPP overexpression or KD had no obvious effects on RNF185 expression and there was no obvious change in RNF185 levels during ER-stress induction (Figs. 4B and S4A, B). Intriguingly, although the level of total GRP78 protein was reduced, the proportion of RNF185-bound GRP78 was increased in HT-29 cells 24 h after TG exposure compared with cells left untreated (controls) or 6 h after TG exposure (Fig. 4C). RNF185 also bound iASPP, but the levels of bound protein were decreased 24 h after TG treatment (Fig. 4C). Therefore, iASPP may interfere with the binding of RNF185 with its substrate GRP78. Indeed, an IP assay showed that binding between GRP78 and RNF185 increased with iASPP KD (Fig. 4D) and decreased with iASPP overexpression (Fig. 4E).

The in vitro IP assay revealed that iASPP directly interacted with RNF185, while binding between iASPP and GRP78 was only detected in the presence of RNF185 and GRP78 addition reduced the binding of RNF185 with iASPP (Fig. 4F). Direct interaction between iASPP and RNF185 in HT-29 cells was also confirmed by PLA (Fig. 4G). In addition, all mutants containing amino acids 1-294 at the N-terminus of iASPP retained the ability to bind to RNF185 binding (Fig. 4H). Intriguingly, the key iASPP-binding region in RNF185 was mapped to its N-terminus, which contains the ring domain (Fig. 4I) that is critical for its binding to GRP78 (Fig. 3F). Moreover, iASPP disrupted RNF185 and GRP78 binding in a dose-dependent manner (Fig. 4J), which is consistent with the data shown in Fig. 4F. Therefore, iASPP binds RNF185 at its ring domain and interferes its binding to GRP78 via a region mapped to (1-96aa).

Downregulation of iASPP upon prolonged ER stress is due to the impaired HuR-mediated iASPP mRNA stabilization

Given its role in controlling the binary ER-stress switch, we investigated the mechanisms underlying iASPP downregulation under ER stress. As shown, iASPP mRNA expression was reduced in a time-dependent manner after TG treatment, which was positively associated with decreased iASPP protein levels (Fig. 5A). However, a luciferase assay showed no obvious change on the reporter activity driven by iASPP promoter after ER-stress stimulation (Fig. S5A). Notably, in ER-stressed cells, the iASPP mRNA half-life was approximately half that of the control cells (Fig. 5B). The bioinformatic tool RBPmap (http://rbpmap.technion.ac.il/) predicted 97 iASPP mRNA RNA-binding proteins (RBPs), of which 25 RBPs were positively associated with iASPP at mRNA levels in colon cancer tissues. We narrowed down the candidates further by choosing potential oncogenes with significantly increased protein levels in colon cancer tissues by analysis of a public data set (The National Cancer Institute's Clinical Proteomic Tumor Analysis Consortium, CPTAC) ($n = 10$) (Fig. S5B). The effects of these genes on iASPP expression were examined by KD of each one (Fig. S5C). Interestingly, only HuR had significant effects on iASPP expression (Fig. S5C). In addition, the protein levels of HuR were decreased by TG in a dose-dependent manner 18 h after TG treatment (Fig. 5C). Restoration of HuR expression rescued TG-mediated iASPP mRNA and protein downregulation (Fig. 5D). KD of HuR reduced iASPP mRNA and protein levels under unstressed conditions (Fig. 5E). TG had little effect on iASPP expression in HuR KD cells (Fig. 5E). Similar phenomena were detected in the presence of two HuR inhibitors, MS-444 and CMLD-2 (Figs. 5F and S5D).

We further dissected the molecular mechanisms of HuR-regulated iASPP mRNA stabilization. First, AU-rich elements (AREs) were predicted in the 3′- untranslated region (UTR) of the iASPP gene. We found that HuR overexpression rescued TG-repressed iASPP-3′-UTR luciferase reporter activity, while HuR KD decreased it (Fig. 5G). Neither TG nor HuR was able to affect the reporter activities of ARE mutants (Fig. 5G), and the effects of HuR inhibitors on luciferase activity were similar to that of HuR KD (Figs. 5H and S5E). Second, UV Cross-Linking and Immunoprecipitation (CLIP) assay showed that HuR was physically associated with iASPP's 3′-UTR and that this association reduced upon TG treatment (Fig. 5I). These data suggest that iASPP expression is decreased as HuR levels reduce during prolonged ER stress, because HuR binds the 3′-UTR of iASPP mRNA and is required for its stability.

HuR/iASPP is associated with GRP78 in vivo in colon cancer tissues

To understand the association of HuR/iASPP with GRP78 in vivo in colon cancer tissues, we collected 40 colon cancer tissue samples and paired adjacent normal controls. GRP78 protein levels were significantly increased in colon cancer tissues compared with normal controls (Fig. 6A, B). This was consistent with our analysis of a public data set (CPTAC) (Fig. S6A). Compared with the significant difference in GRP78 protein levels between the colon cancer samples and matched adjacent controls, the difference in mRNA levels was slight (Figs. 6B and S6B), suggesting that post-transcriptional mechanisms control GRP78 protein output. HuR and iASPP were increased at both the mRNA and protein levels in colon cancer, as shown by analysis of both the in-house samples (Fig. 6A, C, D) and public data set (Fig. S6A, B). In addition, positive correlation between HuR protein and iASPP mRNA or protein levels (Fig. 6E), and between iASPP and GRP78 proteins levels (Fig. 6F), were identified after quantification of the relative expression levels of HuR, iASPP, and GRP78. Furthermore, expression levels of all three proteins were positively correlated with advanced stages of colon cancer (Fig. 6G–I). In contrast, RNF185 expression was unchanged in colon cancer samples compared with normal controls (Figs. 6A, J and S6A, B). As

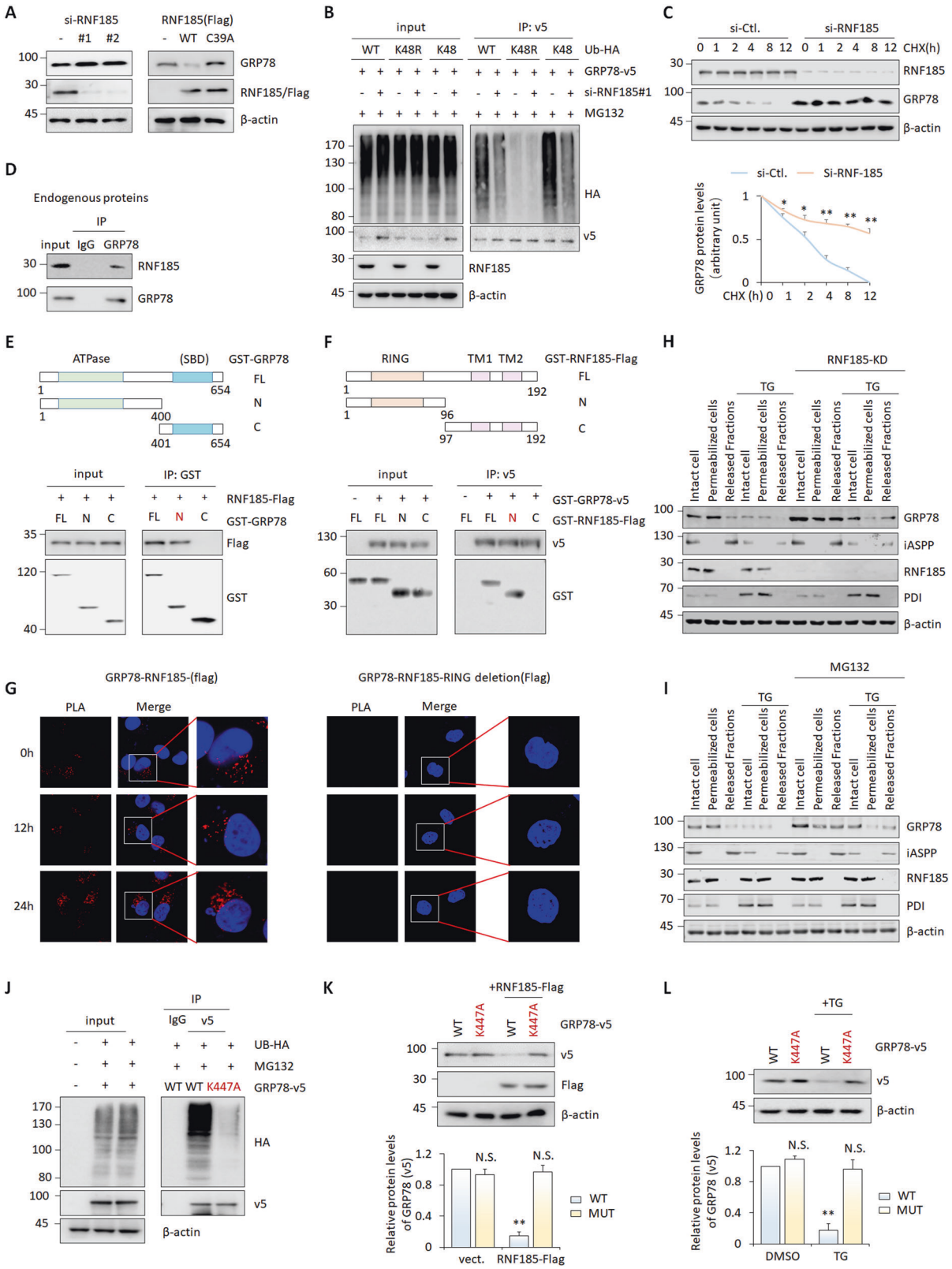

expected, RNF185 was not association with HuR, iASPP, or GRP78 expression (Fig. S6C–E) or with clinical stages of colon cancer (Fig. 6K). These data, combined with the data from in vitro studies, suggest that HuR may contribute iASPP's expression and the subsequent stabilization of GRP78 in vivo.

Chemical or genetic inhibition of HuR/iASPP-GRP78 inhibits tumor growth and sensitizes colon cancer cells to BRAF inhibition

The discovery of the ER-stress switch mechanism inspired us to ask whether such a mechanism is involved in cellular responses to

Fig. 3 GRP78 is a novel substrate of RNF185. A Representative western blot images of GRP78 in RNF185 KD or OE (WT or C39A) HT-29 cells. **B** The Ub-GRP78 was determined by IP/western blot after RNF185 KD and transfection with Ub-HA (WT, K48 or K48R) in the presence of MG132 (20 μM) in HT-29 cells. **C** Representative western blot images of GRP78 and RNF185 in HT29 cells treated with CHX (100 μg/mL). β-actin was used as a loading control. The half-lives of GRP78 were quantified by image J and the data were plotted in the graph shown below. **D** The interaction of endogenous GRP78 and RNF185 in HT-29 cells was determined by IP. The binding between the purified RNF185 and GRP78 (Full length, FL) or its truncated mutants (N-terminus, N or C-terminus, C) (**E**), or the binding between purified GRP78 and FL RNF185 or its truncated mutants (N or C) (**F**) were measured by in vitro IP assay. **G** The direct interaction of GRP78 and RNF185 were detected after transfected with RNF185-Flag-(Full length, FL) or RNF185-Flag-(RING domain deletion) followed by treated with TG by PLA assay in HT-29 cells. Cytosolic GRP78 was detected by the cell permeabilization assay followed by the western blot assay under the treatment of TG and RNF185 KD (**H**) or MG132 (**I**) in HT-29 cells. **J** The Ub-GRP78 (wild type, WT or K447A) was determined by IP/western blot in HT-29 cells in the presence of MG132 (20 μM). Representative western blot images of GRP78-v5 (**K**, **L**), RNF-185-Flag (**K**) in HT-29 cells after the indicated treatments. Values in the control groups were normalized to 1. N.S., not significant; $^{**}P < 0.01$ (**C**, **K**–**L**).

ER-stress-inducing agents. As shown, MTT assay revealed that the IC50 values of TG were decreased by about 2-fold after genetic inhibition of iASPP or GRP78 expression. Double KD of iASPP and GRP78 produced no significant additional effects (Fig. 7A). KD of GRP78 or iASPP increased apoptosis rates, as determined by annexin V/PI staining or caspase 3/7 activity assays, while double KD did not result in further induction of apoptosis (Fig. 7B, C).

To explore the potential clinical application of the newly identified HuR-iASPP-GRP78 axis in cancer treatment, we examined its effects on the sensitivity of cells to the BRAF inhibitor vemurafenib, which has activity connected to ER-stress induction in melanoma, and has been used in the clinic. Vemurafenib treatment increased GRP78 levels in the early stages from 0–24 h, but they decreased over time at 48 h after treatment (Figs. 7D and S7A, B). Restoration of GRP78 expression decreased vemurafenib-induced cell death (Figs. 7E and S7C, D). HuR and iASPP downregulation were only detected at later stages of treatment (after 24 h) (Fig. 7D). iASPP KD or treatment with a HuR inhibitor sensitized the colon cancer cells to vemurafenib (Fig. 7F, G), but the effect of HuR inhibition was compromised by iASPP KD (Fig. 7F, G).

We further evaluated the above findings in vivo in colon cancer xenografts. HT-29 xenograft mice model and drug treatment were shown in Fig. 8A. Inhibition of either iASPP or GRP78 reduced tumor growth, while double KD produced no obvious additional effects (Fig. 8B–D). Inhibition of either iASPP or GRP78 alone, or double KD of iASPP and GRP78, improved the sensitivity of HT-29 xenografts to vemurafenib without obvious effects on body weight (Figs. 8B–D, S7E). iASPP KD and GRP78-KD efficiency was confirmed by WB of xenografts (Fig. 8E). Increased apoptosis contributed to the tumor suppressive effect because caspase 3/7 activity was negatively correlated with tumor growth (Fig. 8F).

We also tested the effect of combining the HuR inhibitor MS-444 with vemurafenib (Fig. 8G). Interestingly, the HT-29 xenografts tolerated the killing effect of vemurafenib (Fig. 8H–J). MS-444 had a mild inhibitory effect on tumor growth (Fig. 8H–J). However, their combination had a significant inhibitory effect on tumor growth (Fig. 8H–J) without having an obvious effect on body weight (Fig. S7F). Examination of the expression levels of iASPP and GRP78 in dissected xenografts revealed that MS-444 reduced iASPP and GRP78 expression (Fig. 8K) and caspase 3/7 activity was increased in combination group compare to single treatment group (Fig. 8L), which is consistent with our in vitro results.

DISCUSSION

Here, we provide novel insight into how iASPP downregulation mediates the transition. Mechanistically, iASPP competes with GRP78 to binding with its E3 ligase RNF185, leading to increased GRP78 stabilization. However, during prolonged ER stress, HuR-mediated iASPP mRNA stabilization and subsequent increased iASPP protein production is significantly impaired, which facilitates RNF185-mediated GRP78 degradation and tips the balance in favor of cell death. Genetic silencing of iASPP or chemical inhibition of HuR significantly promotes GRP78 protein turnover, subsequently inhibiting tumor growth and improving the sensitivity of colon cancer cells to BRAF inhibitor-induced ER stress and cell death (Fig. S8).

Given the dominant role of GRP78 in directing protein re-folding or aiding protein degradation inside the ER, it is unsurprising that transcriptional activation of GRP78 is essential for UPR-induced adaptive survival [24, 25]. In line with this, GRP78 is widely overexpressed at both the mRNA and protein levels in human cancers [26–30], and is associated with drug resistance and poor patient outcomes [31]. Despite being regulated at the transcriptional level, increasing evidence suggests that GRP78 may also be regulated at the post-translational level [23, 32]. Our data demonstrate that the E3 ligase RNF185 is required for GRP78 protein turnover under both basal and ER-stressed conditions. In addition, GRP78 is well-known for its activity in ER. Our data suggested that iASPP-regulated and RNF-185-mediated GRP78 degradation occurs in the cytosol based on the following observations. Firstly, iASPP is localized at cytosol. Secondly, GRP78 is mainly localized at the ER luminal, while its cytosolic fraction is restored by MG132 or genetic silencing of RNF-185. Thirdly, RNF185 is a transmembrane protein localized at ER, which catalyze ubiqutination through its the cytosolic side. It will be also interesting to explore whether HuR/iASPP/Grp78 axis is associated with BRAF mutations in colon cancer samples in future, since both are essential in ER stress regulation.

It is worth noting that the inhibition of GRP78 expression by genetic strategies or nature products sensitizes the responses of cancer cells chemotherapeutics; however, whether dynamic changes in GRP78 levels are involved in regulating the switch remains largely unexplored. Our data reveal that, GRP78 mRNA levels remain high during the ER stress, while its protein levels are increased at adaptive phase, but reduced in the terminal phase via proteasome degradation. These data not only provide an explanation for the discrepancy between the continuous activation of UPR signaling-induced GRP78 transcription and the reduced adaptive ability of cancer cells under prolonged ER stress, but also proved a switch mechanism during prolonged ER stress.

iASPP regulates the switch between the two contrasting phases of the UPR in a GRP78-dependent manner, which influences BRAF inhibitor-induced cell death. This antiapoptotic activity of iASPP is due to is ability to stabilize GRP78, and thus particularly important in the context of ER stress. We previously show that iASPP regulates Ca^{2+} homeostasis by modulating TMCO1 [33]. Given the essential role of Ca^{2+} homeostasis in ER stress, it will be interesting to further explore whether iASPP-TMCO1 axis also contributes to the adaption/death switch. It was recently proposed that oncogenes induce stress adaptations, which may represent a critical weak point that could be targeted by anticancer therapies [34]. iASPP is one such candidate that protects cancer cell from apoptosis induced by various stresses, such as DNA damage [35], oxidative stress [36], or ER stress. iASPP inhibition, in combination with established agents, may elicit a more pronounced anticancer effect; however, no effective inhibitors have been developed to target iASPP to date. Our study reveals a novel mechanism underlying iASPP regulation

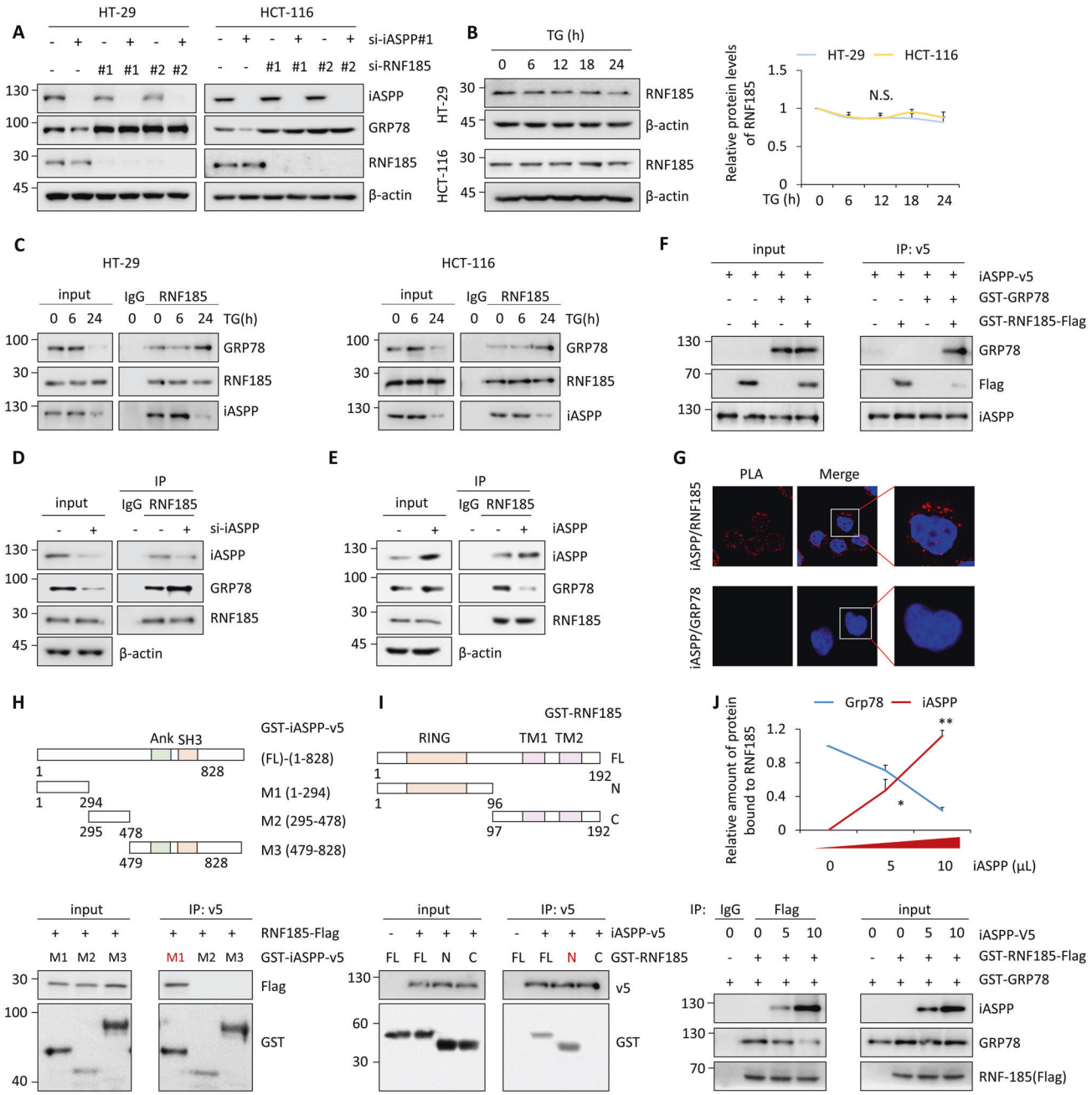

Fig. 4 iASPP competes with GRP78 to bind RNF185. Representative western blot images of GRP78 (**A**), iASPP (**A**) and RNF185 (**A**, **B**) in HT-29 and HCT-116 cells with iASPP KD and/or RNF185 KD (**A**), or treated with 2 ug/mL TG in the indicated time periods (**B**). β-actin was used as a loading control. The bands of RNF185 were quantified by image J and the data were plotted in the graph shown on the right (**B**). The interaction among GRP78, RNF185, iASPP were detected by IP of anti-RNF185 followed by WB assay after treated with TG (**C**), or iASPP KD (**D**) or OE (**E**) in HT-29 and HCT-116 cells. **F** The binding among the purified GRP78 and RNF185 (Flag) and in vitro translated iASPP protein were determined by in vitro IP assay. **G** The direct interaction of iASPP and RNF185 were detected by PLA assay in HT-29 cells. the interaction of iASPP and GRP78 as a negative control. The interactions of purified RNF185 and iASPP fragments (mutant (M)1, M2, M3) (**H**), or iASPP and RNF185 full length and fragments (FL, N, C) (**I**), as indicated in the diagram (H, I), or among RNF185, GRP78 and iASPP with increasing dose of iASPP protein (**J**) were evaluated by in vitro IP assays. The bands of iASPP, GRP78, and RNF185 were quantified by Image J (**J**). Values in the control groups were normalized to 1. N.S., not significant $^{*}P < 0.05$; $^{**}P < 0.01$ (**B**, **J**).

at the post-transcriptional level, HuR-mediated iASPP mRNA stabilization, which may lead to the development of an iASPP inhibitory strategy via chemical inhibition of HuR in cancer treatment, at least in the content of ER stress.

HuR binds to AREs in 3′-UTR region of RNA, resulting in their stabilization [37]. In line with our findings, HuR has been shown to play essential roles in responses to stresses such as hypoxia, glucose starvation, chemotherapy, radiotherapy, and targeted therapies [38–42]. Stress-induced activation of HuR leads to the activation of prosurvival signals and thus confers resistance to many treatments, including PARP (Poly (ADP-ribose) polymerase) inhibitors and the estrogen-receptor inhibitor tamoxifen [43, 44]. Our data provide the first evidence, to the best of our knowledge, that HuR is critical in maintaining the viability of cells under ER stress by protecting iASPP mRNA from degradation. Genetic or chemical inhibition of HuR sensitizes colon cancer cells to BRAF

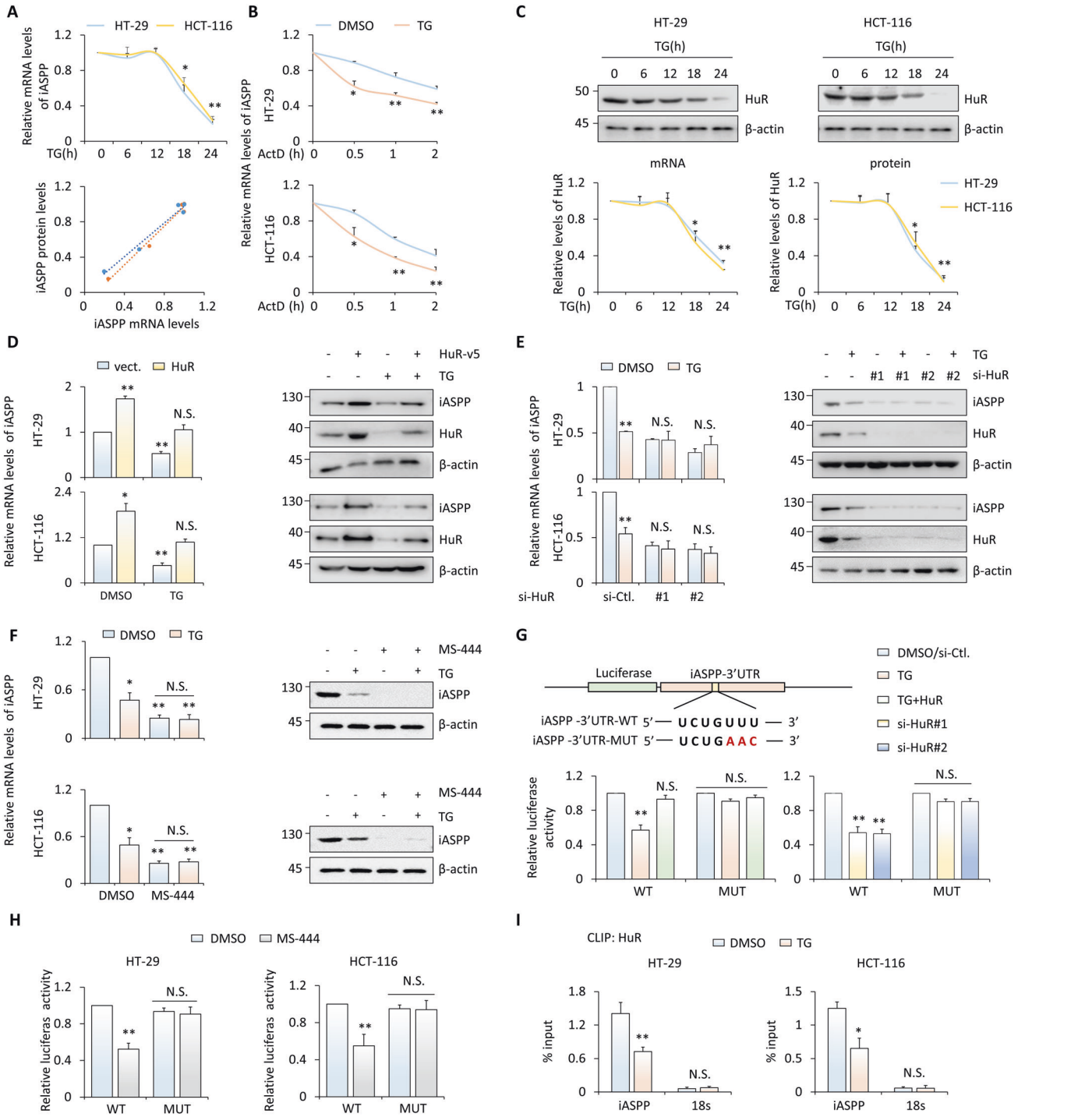

Fig. 5 HuR-mediated iASPP mRNA degradation during prolonged ER stress. The mRNA levels of iASPP were detected by qRT-PCR assays in HT-29 and HCT-116 cells treated with TG (**A**), or with ActD (**B**). The correlation of mRNA and protein levels of iASPP was showed in the line graph (**A**). Representative western blot images of HuR (**C**–**E**) or iASPP (**D**–**F**) in HT-29 and HCT-116 cells treated with TG (**C**), or with HuR OE (**D**) or KD (**E**) followed by the TG treatment, or treating with TG and/or MS-444 (**F**). β-actin was used as a loading control. The mRNA levels of iASPP were detected by qRT-PCR assays in parallel with western blot analysis (**D**–**F**). The luciferase plasmids of iASPP-3′UTR (WT or mutant, MUT) were generated as shown in **G**. The luciferase activities were measured by luciferase reporter assays in HT-29 and HCT-116 cells with HuR OE or KD, in the presence or absence of TG (**G**), or with MS-444 treatments (**H**). **I** The binding of HuR and iASPP 3′UTR was detected by CLIP/qRT-PCR assays in HT-29 and HCT-116 cells after TG treatment. 18S was used as the negative control. Values in the control groups were normalized to 1. N.S., not significant $^{*}P < 0.05$; $^{**}P < 0.01$ (**A**–**I**).

inhibitor-induced and ER-stress-related cell death. Further research is necessary to test the effects of HuR inhibitors in combination with other ER-stress-inducing treatments in addition to BRAF inhibitors.

In summary, this study provide evidence of how cells switch to the death phase by attenuating the protective UPR mediated by GRP78 through the HuR-iASPP axis. Targeting iASPP or HuR promotes RNF185-induced GRP78 degradation, and sensitizes

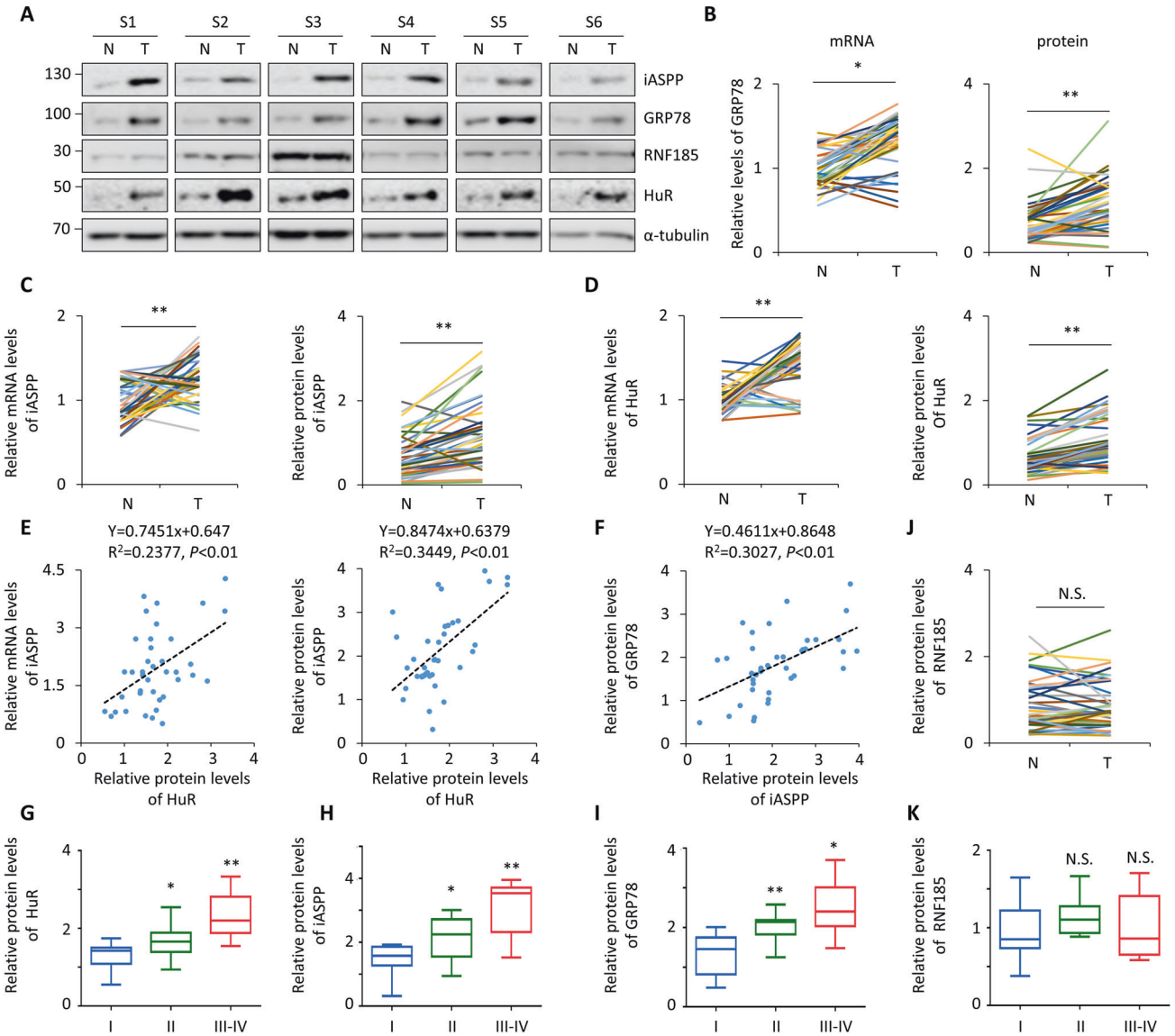

Fig. 6 HuR/iASPP is associated with GRP78 in vivo in colon cancer tissues. A, **B–D**, **J** Representative western blot images of iASPP, GRP78, RNF185, HuR protein in 40 pairs of human colon cancer tissues (T) and their matched adjacent normal controls (N). α-tubulin was used as a loading control (**A**). Western blots bands were quantified by Image J and the data were shown in the graphs (**B–D**, **J**). The mRNA levels of GRP78 (**B**), iASPP (**C**) and HuR (**D**) were detected by qRT-PCR assays. **(E, F)** The scatter diagram showed the lineal correlation of HuR protein/iASPP mRNA ($P < 0.01$, **E**), HuR protein/iASPP protein ($P < 0.01$, **E**) or iASPP protein/GRP78 protein ($P < 0.01$, **F**) in colon cancer tissues. The correlation between HuR (**G**), iASPP (**H**), GRP78 (**I**) and RNF185 (**K**) protein levels and tumor stages was shown in the Box plot.

colon cancer cells to BRAF inhibitor (ER-stress inducer)-induced apoptosis both in vitro and in vivo.

MATERIALS AND METHODS

Tissue samples

The pairs of human colorectal cancer tissues and corresponding adjacent controls were acquired from the Third Affiliated Hospital of Harbin Medical University in China ($n = 40$). The informed consent was obtained from all patients. After the surgery, all samples were collected in liquid nitrogen immediately. The study has been approved by the Research Ethics Committee of Harbin Medical University, China.

Xenografted tumor model in vivo

The female nude mice between 4 and 5 weeks were purchased from Beijing HFK Bioscience Co., Ltd. All animal procedures were performed according to protocols approved by the Rules for Animal Experiments published by the Chinese Government (Beijing, China) and approved by the Research Ethics Committee of Harbin Institute of Technology, China. The equal number of cells were transplanted subcutaneously into either side of flank of the same female nude mouse ($n = 5$/group). The tumor size or body weights of mice were measured weekly. After 4 weeks, the tumors of mice were isolated, photographed and weighed and the tissues were subjected to the following assays. The mice were treatedvemurafenib (PLX4720) (50 mg/kg, oral gavage, twice a day for 4 weeks) and/or MS-444 (25 mg/kg, intraperitoneally, every other day for 4 weeks) with PBS as controls.

Cell line and transfection

Human colorectal cancer cell lines HT-29, HCT-116, bladder cancer cell line T24 and cervical cancer cell line HeLa were authenticated by the suppliers. Cells were cultured with Dulbecco's modified Eagle's medium (DMEM) or RPMI-1640 medium (Gibco, Carlsbad, CA, USA), supplemented with 10% (v/v) fetal bovine serum (Biological industries), and grown in the humidified incubator at 37 °C with 5% CO_2.

Lentilvirus expressing the short hairpin iASPP (shiASPP), shGRP78 or scrambled shRNA (shnone) were packed in 293 T cells. 48–72 h after

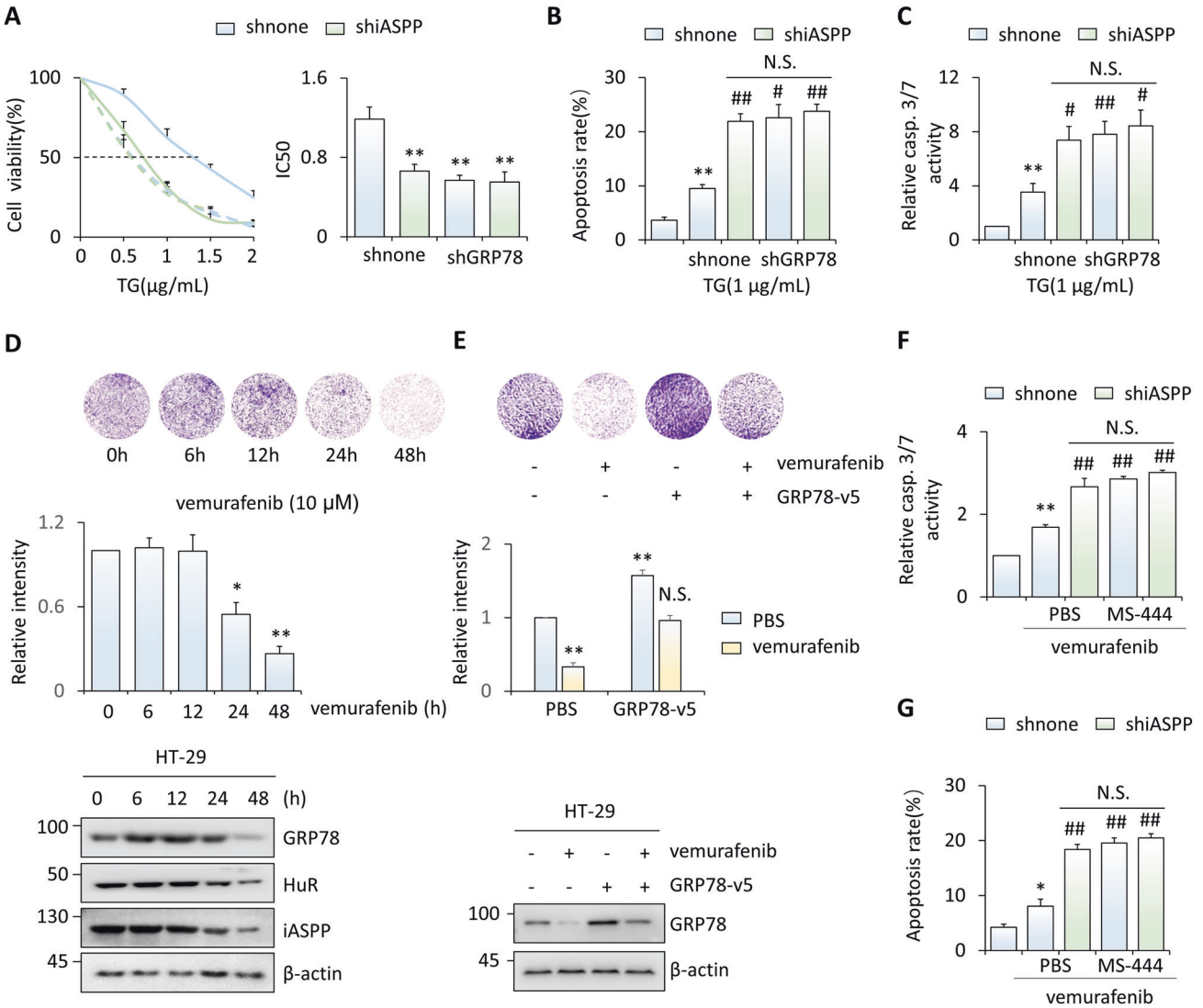

Fig. 7 Chemical or genetic inhibition of HuR/iASPP-GRP78 inhibits sensitizes colon cancer cells to BRAF inhibition in vitro. A Cell viability was determined by MTT assay and the IC50 was showed in bar graph in iASPP and/or GRP78 KD cells in the indicated TG treatment. The apoptosis levels were detected by Annexin V/PI staining (**B**, **G**) and caspase 3/7 activity (**C**, **F**) assays by TG treatment in iASPP and/or GRP78 KD HT-29 cells (**B**, **C**), or vemurafenib treatment in HT-29 cells (**F**, **G**). Representative crystal violet staining images, quantification of images, representative western blot images of GRP78, iASPP and HuR in HT-29 cells exposed to vemurafenib for the different time periods (**D**) or in GRP78-v5 overexpressing HT-29 cells in the presence of vemurafenib (**E**). Line graphs (**A**) or Bar graphs (**A**–**G**) represent the mean ± SEM from three independent assays. $^{*}P < 0.05$; $^{**}P < 0.01$; N.S. not significant. (**A**–**G**). $^{\#}P < 0.05$; $^{\#\#}P < 0.01$ compared to TG or vemurafenib treatment control (**B**, **C**, **F**, **G**).

transfection, the virus was collected and infected the target cells with polybrene (10 μg/ml). The stable cell lines were selected by limiting dilution. The indicated siRNA sequences were listed in Supplemental Table 1.

RNA extraction and quantitative reverse transcription (qRT) PCR

Total RNA from cancer cells or tissues was isolated by using the Trizol (Invitrogen, USA) and performed the reverse transcription by GoScriptTM Reverse Transcription System (Promega, USA) according to the manufacturer's instruction. The resulting cDNA were subjected to the Quantitative real-time PCR by the SYBR Premix Ex Tag II (TaKaRa, Japan) in the Vii7 real-time PCR (Applied Biosystems, USA). Gene expressions were analyzed by $2^{-\Delta\Delta}$CT method. The GAPDH was used as an internal control. The sequences of primer were listed in Supplemental Table 2.

Western blot assay

Cancer cells or tissues were lysed by using urea buffer (2M Thiourea, 4% CHAPS, 40 mM Tris-Base, 40 mM DTT, 2% Pharmalyte) and sonicated to break DNA to obtain the total protein. The indicated protein bands were visualized by ECL. Images were detected by Image studio system (ECL, LI-COR, Lincoln, Georgia, USA) and analyzed by Image J software. The corresponding antibodies used in this study were listed in Supplemental Table 3.

Luciferase activity assay

The iASPP promoter or 3′UTR sequence was inserted into PGL3-basic or pMIR-REPORT luciferase reporter plasmid, respectively. The pMIR-iASPP-3′UTR mutant (MUT) were cloned by using mutagenesis kit according to the manufacturer's introduction using pMIR-iASPP-3′UTR as the template. Cells were transfected with a mixture containing the indicated luciferase reporters plasmids and Renilla luciferase by using Lipofectamine 2000. The luciferase activities were measured using Dual-Luciferases Reporter Assay System (Promega, Madison, WI, USA) in Fluorescence microplate reader at absorbance of 528 nm for luciferase and 405 nm for renilla. The relative luciferase activities in the controls were normalized with the Renilla luciferase activities.

Purification of recombinant protein

The indicated gene sequences were cloned into the pGEX-6p-1 expression vector. Protein expression was induced in the *E. coli* strain BL21 (DE3) by adding 0.1 mM isopropyl β-d-1-thiogalactopyranoside (IPTG). The recombinant protein were purified by BeyoGold™ GST-tag Purification Resin

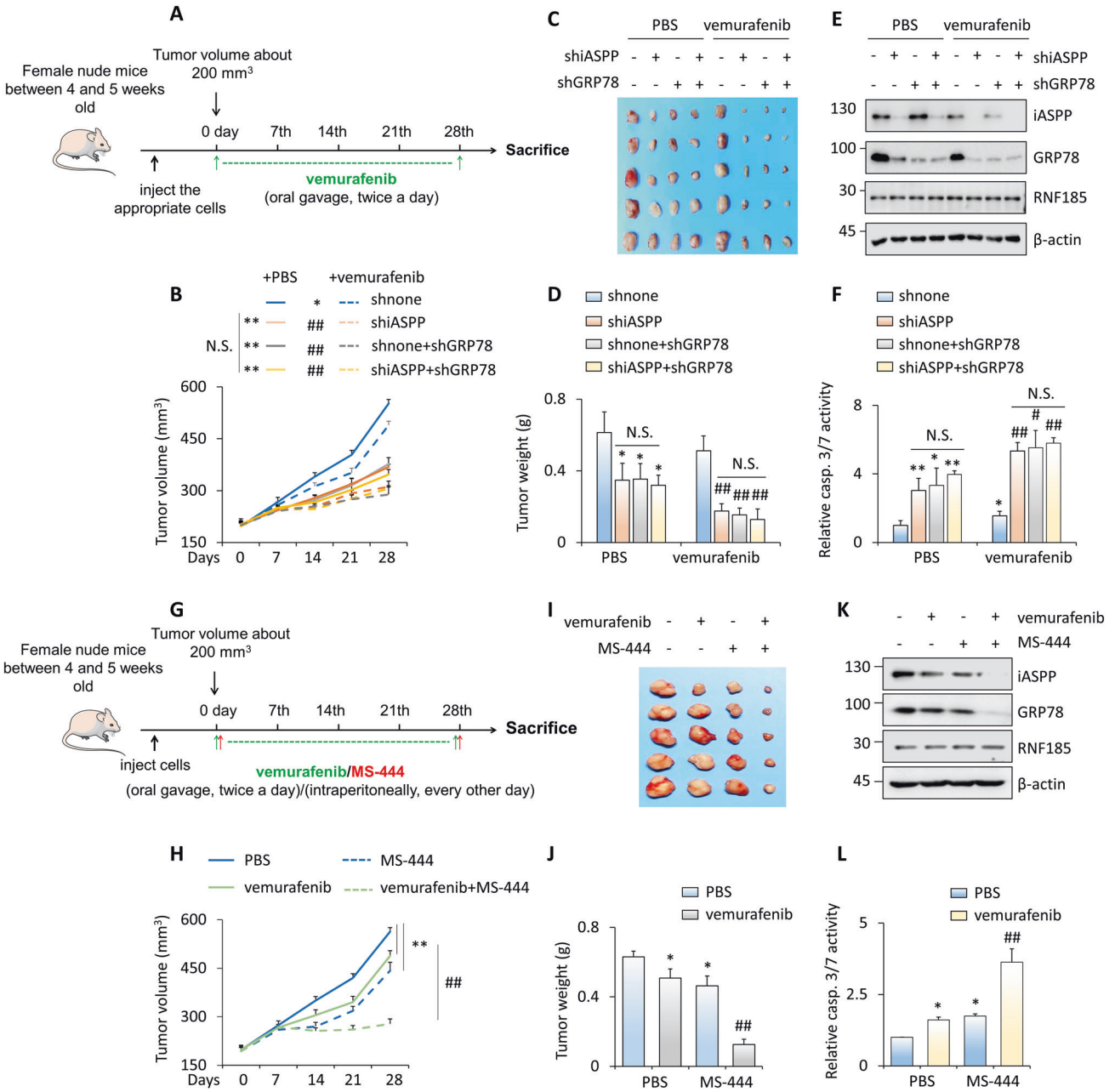

Fig. 8 Chemical or genetic inhibition of HuR/iASPP-GRP78 sensitizes colon cancer cells to BRAF inhibition in vivo. The schematic diagram of the treatment strategies for the xenograft bearing nude mice. HT-29 cells with different genetic modifications were inoculated into nude mice and then subjected to the PBS or vemurafenib treatment (**A**). HT-29 cells were inoculated into nude mice and then subjected to the vemurafenib and/or MS-444 treatments (**G**). HT-29 xenograft volumes in the indicated time periods (**B**, **H**), tumor images (**C**, **I**) or tumor weight (**D**, **J**) were presented with the indicated treatments. Representative western blot images of iASPP, GRP78, and RNF185 (**E**, **K**) and caspase 3/7 activity (**F**, **L**) of the indicated xenografts. β-actin was used as a loading control. The average values are present in the graphs (**B**, **D**, **H**, **J**) (means ± SD) ($n = 5$ for each group). $^{*}P < 0.05$; $^{**}P < 0.01$; N.S. not significant; $^{\#}P < 0.05$; $^{\#\#}P < 0.01$ compared to vemurafenib treatment control (**D**, **F**).

(Beyotime, China) and elucidated by elution buffer. The protein purity was validation by comassie brilliant blue staining.

In vitro translation

Briefly, the mixture included 1 μg indicated plasmid, 1 μL unlabeled methionine (1 mM) and 40 μL TNT® Quick Master Mix in a total volume 50 μL was incubated at 30 °C for 90 min according to the manufacturer's instructions (L1171, Promega). The resulting proteins were ready for in vitro IP assays, as described below.

Immunoprecipitation (IP) assay

Cells lysed in NETN buffer (50 mM Tris-HCl pH 8.0, 150 mM NaCl,1% NP-40, 1 mM EDTA) supplemented with Proteinase Inhibitor Cocktail (MedChemExpress, USA) or in vitro purified or translated proteins were pre-cleaned by protein G sepharose beads (GE Healthcare, USA) at 4 °C. The resulting mixtures were incubated with the blocked protein G sepharose and the primary antibodies or the control IgG on a rotating wheel at 4 °C overnight. The beads were collected and washed four times with the cold NETN buffer followed by western blot assays.

UV-cross-linking RNA-IP (CLIP)

The interaction between RNA and protein were determined by CLIP assay as described [45]. Briefly, the cells were subjected to the UV cross-link at 400 mJ/cm^2 followed by lysis in a buffer supplemented with the fresh Protease Inhibitor Cocktail and RNase inhibitor (Thermo Fisher, Rockford,

IL). The pre-cleaned lysates were incubated with the indicated antibody or the control IgG on a rotating wheel at 4 °C overnight. The immunoprecipitated RNA was elucidated and analyzed by qRT-PCR for the target RNA of interest by qRT-PCR.

Ubiquitination assay

Cells were transfected with the indicated plasmids and treated with 20 μM MG132 (MedChemExpress) for 6 h before harvest. The cells were lysed in lysis buffer containing 2% SDS, 150 mM NaCl, 10 mM Tris-HCl, pH 8.0 supplemented with Protease Inhibitor Cocktail (MedChemExpress) freshly. The resulting lysates were subjected to the IP and western blot assays.

Proximity Ligation Assay (PLA)

The PLA assays were performed using Duolink® reagents (Sigma-Aldrich) according to the manufacturer's instructions. The signal was amplified by ligation and detected by confocal microscope (LSM880).

Cell permeabilization

Digitonin can selectively permeabilize the plasma membrane rather than the organelle membrane, as previously reported [46]. Briefly, the indicated cells were collected, half of cells were resuspended in transport buffer (20 mM HEPES, pH 7.4, 110 mM potassium acetate, 2 mM magnesium acetate, 0.5 mM EGTA) supplemented with proteinase inhibitor cocktail. Cell permeabilization assay was performed in 0.01% digitonin for 5 min on ice. After centrifugation, the pellet and supernatant were collected to further western blot assay.

ER fractionation assay

The assay was performed as described previously [47]. Briefly, cells were lysed with MTE buffer (270 mM D-mannitol, 10 mM Tris-Cl, pH7.4, 0.1 mM EDTA) supplemented with proteasome inhibitor cocktail (MedChemExpress, USA) and further disrupted by sonication. The lysate was centrifuged at 1400 *g*, 4 °C for 10 min to yield nucleus-enriched pellet. The supernatant was subjected to another round of centrifuge at 15,000 *g* at 4 °C for 10 min to separate crude ER containing supernatant from crude mitochondria (pellet). The supernatant was then loaded on a sucrose gradient and centrifuged at 152,000 *g* at 4 °C for 70 min. The top part of solution was collected as the cytosol and the median portion observed "white band" was collected by syringe and centrifuged at 126,000 *g*, 4 °C for additionally 45 min. The pellet was obtained as the ER fraction. All collected lysates were subjected to western blot analysis.

XBP1 splicing assay

XBP1 splicing assay was performed by PCR. Briefly, the indicated primers were used to amplify both unspliced and spliced sequence of human XBP1 mRNA to generate the products of 289 and 263 bp, respectively. The resulting products were showed on 2% agarose gels with ethidium bromide staining. The primer sequence of XBP1 was listed in Table S1.

MTT assay

Briefly, the same amounts of cells was planted in 96 well plates. After the indicated treatment, the cells were incubated with MTT solution (0.5 mg/mL) for 4 h at 37 °C and formazan was dissolved with 100 μL DMSO. The absorbance of 490 nm was measured by Microplate Reader (Tecan Austria GmbH 5082, Grodig, Austria).

Crystal violet staining

Cells after the indicated treatments were fixed with 4% formaldehyde at room temperature for 30 min, and then stained with 0.1% crystal violet solution for 20 min. After washed four times with PBS, the plates were photographed and the images were quantified.

Apoptosis assay

The apoptosis assay were performed by Annexin V and propidium idodide (PI) staining according to the manufacturer's instructions (Sungene, Tianjin). The positive stained cells were analyzed by flow cytometry (FCM) within 1 h. All reactions were carried out in the dark.

Caspase 3/7 activity assay

The caspase 3/7 activity was measured using Caspase-Glo 3/7 Assay Systems (Promega) according to the manufacturer's instructions. The assay was repeated for three times independently, which was represented as a fold-increase of fluorescence calculated by comparing to untreated controls.

Statistical analysis

Statistical analysis was performed by the GraphPad software, version 6.0. The experiments were repeated independently at least for three times. Data were showed as means ± standard error of the means (SEM) or standard Deviation (SD). Student *t*-test was used to analyze the statistical significance between the two groups. $P < 0.05$ were considered as significant.

DATA AVAILABILITY

All data are present in the manuscript and the Supplementary Materials. Additional data related to this paper may be requested from the corresponding author.

REFERENCES

1. Chen X, Cubillos-Ruiz JR. Endoplasmic reticulum stress signals in the tumour and its microenvironment. Nat Rev Cancer. 2021;21:71–88.
2. Clarke HJ, Chambers JE, Liniker E, Marciniak SJ. Endoplasmic reticulum stress in malignancy. Cancer Cell. 2014;25:563–73.
3. Hetz C, Zhang K, Kaufman RJ. Mechanisms, regulation and functions of the unfolded protein response. Nat Rev Mol Cell Biol. 2020;21:421–38.
4. Walter P, Ron D. The unfolded protein response: from stress pathway to homeostatic regulation. Science. 2011;334:1081–6.
5. Hetz C, Chevet E, Harding HP. Targeting the unfolded protein response in disease. Nat Rev Drug Discov. 2013;12:703–19.
6. Blackwood EA, Hofmann C, Santo Domingo M, Bilal AS, Sarakki A, Stauffer W, et al. ATF6 regulates cardiac hypertrophy by transcriptional induction of the mTORC1 activator, Rheb. Circ Res. 2019;124:79–93.
7. Dong H, Adams NM, Xu Y, Cao J, Allan DSJ, Carlyle JR, et al. The IRE1 endoplasmic reticulum stress sensor activates natural killer cell immunity in part by regulating c-Myc. Nat Immunol. 2019;20:865–78.
8. Wang M, Kaufman RJ. Protein misfolding in the endoplasmic reticulum as a conduit to human disease. Nature 2016;529:326–35.
9. Hetz C. The unfolded protein response: controlling cell fate decisions under ER stress and beyond. Nat Rev Mol Cell Biol. 2012;13:89–102.
10. Wei MC, Zong WX, Cheng EH, Lindsten T, Panoutsakopoulou V, Ross AJ, et al. Proapoptotic BAX and BAK: a requisite gateway to mitochondrial dysfunction and death. Science. 2001;292:727–30.
11. Marciniak SJ, Yun CY, Oyadomari S, Novoa I, Zhang Y, Jungreis R, et al. CHOP induces death by promoting protein synthesis and oxidation in the stressed endoplasmic reticulum. Genes Dev. 2004;18:3066–77.
12. Zhu X, Zhang J, Sun H, Jiang C, Dong Y, Shan Q, et al. Ubiquitination of inositol-requiring enzyme 1 (IRE1) by the E3 ligase CHIP mediates the IRE1/TRAF2/JNK pathway. J Biol Chem. 2014;289:30567–77.
13. Hetz C, Bernasconi P, Fisher J, Lee A-H, Bassik MC, Antonsson B, et al. Proapoptotic BAX and BAK modulate the unfolded protein response by a direct interaction with IRE1alpha. Science. 2006;312:572–6.
14. Pagliarini V, Giglio P, Bernardoni P, De Zio D, Fimia GM, Piacentini M, et al. Downregulation of E2F1 during ER stress is required to induce apoptosis. J Cell Sci. 2015;128:1166–79.
15. Ge W, Zhao K, Wang X, Li H, Yu M, He M, et al. iASPP is an antioxidative factor and drives cancer growth and drug resistance by competing with Nrf2 for Keap1 binding. Cancer Cell. 2017;32:561–73.
16. Bergamaschi D, Samuels Y, O'Neil NJ, Trigiante G, Crook T, Hsieh J-K, et al. iASPP oncoprotein is a key inhibitor of p53 conserved from worm to human. Nat Genet. 2003;33:162–7.
17. Liu K, Chen W, Lei S, Xiong L, Zhao H, Liang D, et al. Wild-type and mutant p53 differentially modulate miR-124/iASPP feedback following pohotodynamic therapy in human colon cancer cell line. Cell Death Dis. 2017;8:e3096.
18. Cheng Z, Dai Y, Pang Y, Jiao Y, Zhao H, Zhang Z, et al. Enhanced expressions of FHL2 and iASPP predict poor prognosis in acute myeloid leukemia. Cancer Gene Ther. 2019;26:17–25.
19. Lu M, Breyssens H, Salter V, Zhong S, Hu Y, Baer C, et al. Restoring p53 function in human melanoma cells by inhibiting MDM2 and cyclin B1/CDK1-phosphorylated nuclear iASPP. Cancer Cell. 2013;23:618–33.
20. Wang Q-C, Zheng Q, Tan H, Zhang B, Li X, Yang Y, et al. TMCO1 is an ER Ca(2+) load-activated Ca(2+) channel. Cell. 2016;165:1454–66.
21. Cubillos-Ruiz JR, Bettigole SE, Glimcher LH. Tumorigenic and immunosuppressive effects of endoplasmic reticulum stress in cancer. Cell. 2017;168:692–706.
22. Yong J, Johnson JD, Arvan P, Han J, Kaufman RJ. Therapeutic opportunities for pancreatic β-cell ER stress in diabetes mellitus. Nat Rev Endocrinol. 2021;17:455–67.

23. Chang YW, Tseng CF, Wang MY, Chang WC, Lee CC, Chen LT, et al. Deacetylation of HSPA5 by HDAC6 leads to GP78-mediated HSPA5 ubiquitination at K447 and suppresses metastasis of breast cancer. Oncogene. 2016;35:1517–28.
24. Shi-Chen Ou D, Lee S-B, Chu C-S, Chang L-H, Chung B-C, Juan L-J. Transcriptional activation of endoplasmic reticulum chaperone GRP78 by HCMV IE1-72 protein. Cell Res. 2011;21:642–53.
25. Lee AS. Glucose-regulated proteins in cancer: molecular mechanisms and therapeutic potential. Nat Rev Cancer. 2014;14:263–76.
26. Dai R-Y, Chen Y, Fu J, Dong L-W, Ren Y-B, Yang G-Z, et al. p28GANK inhibits endoplasmic reticulum stress-induced cell death via enhancement of the endoplasmic reticulum adaptive capacity. Cell Res. 2009;19:1243–57.
27. Arap MA, Lahdenranta J, Mintz PJ, Hajitou A, Sarkis AS, Arap W, et al. Cell surface expression of the stress response chaperone GRP78 enables tumor targeting by circulating ligands. Cancer Cell. 2004;6:275–84.
28. Shuda M, Kondoh N, Imazeki N, Tanaka K, Okada T, Mori K, et al. Activation of the ATF6, XBP1 and grp78 genes in human hepatocellular carcinoma: a possible involvement of the ER stress pathway in hepatocarcinogenesis. J Hepatol. 2003;38:605–14.
29. Du T, Li H, Fan Y, Yuan L, Guo X, Zhu Q, et al. The deubiquitylase OTUD3 stabilizes GRP78 and promotes lung tumorigenesis. Nat Commun. 2019;10:2914.
30. Winder T, Bohanes P, Zhang W, Yang D, Power DG, Ning Y, et al. GRP78 promoter polymorphism rs391957 as potential predictor for clinical outcome in gastric and colorectal cancer patients. Ann Oncol. 2011;22:2431–9.
31. Roué G, Pérez-Galán P, Mozos A, López-Guerra M, Xargay-Torrent S, Rosich L, et al. The Hsp90 inhibitor IPI-504 overcomes bortezomib resistance in mantle cell lymphoma in vitro and in vivo by down-regulation of the prosurvival ER chaperone BiP/Grp78. Blood. 2011;117:1270–9.
32. Kim S-Y, Kim HJ, Kim H-J, Kim DH, Han JH, Byeon HK, et al. HSPA5 negatively regulates lysosomal activity through ubiquitination of MUL1 in head and neck cancer. Autophagy. 2018;14:385–403.
33. Zheng S, Zhao D, Hou G, Zhao S, Zhang W, Wang X, et al. iASPP suppresses Gp78-mediated TMCO1 degradation to maintain Ca homeostasis and control tumor growth and drug resistance. Proc Natl Acad Sci USA. 2022;119:e2111380119.
34. Gorrini C, Harris IS, Mak TW. Modulation of oxidative stress as an anticancer strategy. Nat Rev Drug Discov. 2013;12:931–47.
35. Kramer D, Schön M, Bayerlová M, Bleckmann A, Schön MP, Zörnig M, et al. A pro-apoptotic function of iASPP by stabilizing p300 and CBP through inhibition of BRMS1 E3 ubiquitin ligase activity. Cell Death Dis. 2015;6:e1634.
36. Wang C-Y, Zhang Q, Xun Z, Yuan L, Li R, Li X, et al. Increases of iASPP-Keap1 interaction mediated by syringin enhance synaptic plasticity and rescue cognitive impairments via stabilizing Nrf2 in Alzheimer's models. Redox Biol. 2020;36:101672.
37. Stellos K, Gatsiou A, Stamatelopoulos K, Perisic Matic L, John D, Lunella FF, et al. Adenosine-to-inosine RNA editing controls cathepsin S expression in atherosclerosis by enabling HuR-mediated post-transcriptional regulation. Nat Med. 2016;22:1140–50.
38. Zhang L-F, Lou J-T, Lu M-H, Gao C, Zhao S, Li B, et al. Suppression of miR-199a maturation by HuR is crucial for hypoxia-induced glycolytic switch in hepatocellular carcinoma. EMBO J. 2015;34:2671–85.
39. Wu M, Tong CWS, Yan W, To KKW, Cho WCS. The RNA binding protein HuR: A promising drug target for anticancer therapy. Curr Cancer Drug Targets. 2019;19:382–99.
40. Lin G-L, Ting H-J, Tseng T-C, Juang V, Lo Y-L. Modulation of the mRNA-binding protein HuR as a novel reversal mechanism of epirubicin-triggered multidrug resistance in colorectal cancer cells. PLoS One. 2017;12:e0185625.
41. Zhang R, Wang J. HuR stabilizes TFAM mRNA in an ATM/p38-dependent manner in ionizing irradiated cancer cells. Cancer Sci. 2018;109:2446–57.
42. Siang DTC, Lim YC, Kyaw AMM, Win KN, Chia SY, Degirmenci U, et al. The RNA-binding protein HuR is a negative regulator in adipogenesis. Nat Commun. 2020;11:213.
43. Chand SN, Zarei M, Schiewer MJ, Kamath AR, Romeo C, Lal S, et al. Post-transcriptional regulation of mRNA by HuR facilitates DNA repair and resistance to PARP inhibitors. Cancer Res. 2017;77:5011–25.
44. Tan S, Ding K, Chong Q-Y, Zhao J, Liu Y, Shao Y, et al. Post-transcriptional regulation of ERBB2 by miR26a/b and HuR confers resistance to tamoxifen in estrogen receptor-positive breast cancer cells. J Biol Chem. 2017;292:13551–64.
45. Zhang Y, He Q, Hu Z, Feng Y, Fan L, Tang Z, et al. Long noncoding RNA LINP1 regulates repair of DNA double-strand breaks in triple-negative breast cancer. Nat Struct Mol Biol. 2016;23:522–30.
46. Afshar N, Black BE, Paschal BM. Retrotranslocation of the chaperone calreticulin from the endoplasmic reticulum lumen to the cytosol. Mol Cell Biol. 2005;25:8844–53.
47. Park SJ, Jeong J, Park Y-U, Park K-S, Lee H, Lee N, et al. Disrupted-in-schizophrenia-1 (DISC1) regulates endoplasmic reticulum calcium dynamics. Sci Rep. 2015;5:8694.

AUTHOR CONTRIBUTIONS

YH designed the experiments and wrote the paper. SZ, XW, HL, DZ, and QL performed the experiments and analyzed the data. LL collected clinical samples. QJ performed the bioinformatic analysis.

FUNDING

The work was funded by the National Key R & D Program of China (2022YFA1105200), Interdisciplinary Research Foundation of HIT, National Nature Science Foundation (Nos. 82025027, 82150115, 31871389 and 32000517), and Nature Science Foundation of Heilongjiang Province (No. YQ2021C024).

COMPETING INTERESTS

The authors declare no competing interests.

ETHICS

The study for human colon cancer samples has been approved by the Research Ethics Committee of Harbin Medical University, China. All animal procedures were performed according to protocols approved by the Rules for Animal Experiments published by the Chinese Government (Beijing, China) and approved by the Research Ethics Committee of Harbin Institute of Technology, China.

ADDITIONAL INFORMATION

Supplementary information The online version contains supplementary material available at https://doi.org/10.1038/s41418-022-01086-w.

Correspondence and requests for materials should be addressed to Li Li or Ying Hu.

Reprints and permission information is available at http://www.nature.com/reprints

Publisher's note Springer Nature remains neutral with regard to jurisdictional claims in published maps and institutional affiliations.